ARTICLE

doi:10.1038/nature11131

Dimensionality of consumer search space drives trophic interaction strengths

Samraat Pawar[1], Anthony I. Dell[1,2] & Van M. Savage[1,3,4]

Trophic interactions govern biomass fluxes in ecosystems, and stability in food webs. Knowledge of how trophic interaction strengths are affected by differences among habitats is crucial for understanding variation in ecological systems. Here we show how substantial variation in consumption-rate data, and hence trophic interaction strengths, arises because consumers tend to encounter resources more frequently in three dimensions (3D) (for example, arboreal and pelagic zones) than two dimensions (2D) (for example, terrestrial and benthic zones). By combining new theory with extensive data (376 species, with body masses ranging from 5.24×10^{-14} kg to 800 kg), we find that consumption rates scale sublinearly with consumer body mass (exponent of approximately 0.85) for 2D interactions, but superlinearly (exponent of approximately 1.06) for 3D interactions. These results contradict the currently widespread assumption of a single exponent (of approximately 0.75) in consumer–resource and food-web research. Further analysis of 2,929 consumer–resource interactions shows that dimensionality of consumer search space is probably a major driver of species coexistence, and the stability and abundance of populations.

Understanding how physical differences between habitats, such as differences in precipitation, temperature and spatial dimensionality, affect trophic interactions is key to predicting stability and diversity in ecological systems[1–6]. By assuming a simple relationship between consumption rate (energy acquisition) and metabolic rate (energy use), most studies assume that per-capita consumption rates scale with consumer body size (m) to an exponent of approximately 0.75, irrespective of taxon, environment or dimensionality[7–13]. Consequently, mass-specific production rates[8,14] scale as $m^{-0.25}$, including biomass flow rate and per-link trophic interaction strengths in food webs[10,11,13,15,16]. Deviations from quarter-power scaling can arise for at least two reasons. First, foraging is constrained by traits, such as length of locomotory appendages or visual acuity, that do not scale directly with metabolic rate[8,17–20]. Second, species interactions in the field do not occur under the idealized conditions at which metabolic and ingestion rates are usually measured, in which individuals are not foraging, growing or reproducing[8,18,19]. Therefore, consumption-rate scaling may be more closely tied to field or maximal metabolic rate (exponent greater than 0.85), rather than resting metabolic rate (exponent of approximately 0.75)[8,21].

From a biomechanical perspective, both non-metabolic and metabolic constraints on consumption rate should depend on the habitat's spatial dimensionality because it strongly influences the energetic costs of locomotion (for example, to overcome gravity)[18,19] and the probability either of a consumer detecting a resource or vice versa[17,20]. Indeed, over two decades ago, habitat dimensionality was proposed as a major factor driving food-web structure and ecosystem dynamics[1,4,22]. Subsequent studies have further elucidated the effects of habitat dimensionality[3,6,23–25]. Notably, previous models suggest that grazers (one type of consumer; Fig. 1 and Supplementary Fig. 1) are constrained by how resources are distributed in space[3,24,25]. These studies are foundational, but do not apply to the full diversity of foraging strategies and interactions in natural communities.

Here we show that shifting focus from dimensionality of the habitat[3,4,6,23–25] to the dimensionality of each trophic interaction yields a new, mechanistic theory for trophic interaction strengths (Figs 1 and 2). Our approach allows both 2D and 3D interactions within the same habitat to be considered, and can be applied to the wide range of foraging strategies found in nature (Fig. 1 and Supplementary Fig. 1). To test our predictions, we compiled a data set that contains a per-capita consumption rate of 255 consumer–resource interactions covering 230 species, 12 orders of magnitude in body size, and aquatic (189 interactions) as well as terrestrial (66 interactions) habitats (Methods).

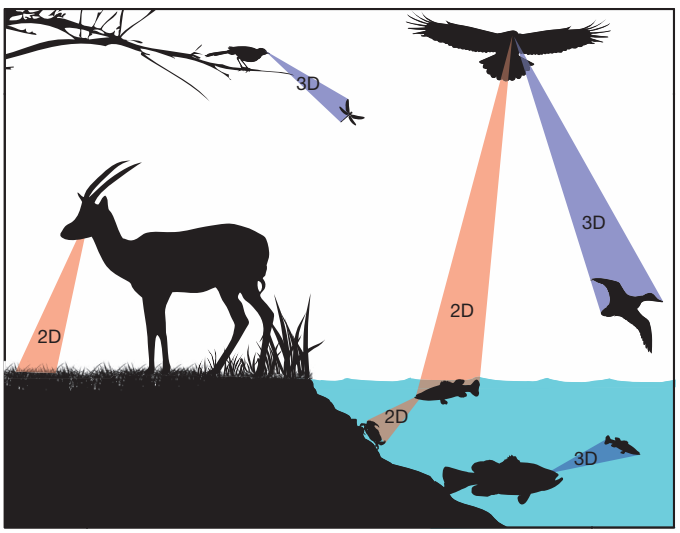

Figure 1 | Consumer–resource interactions can be classified by dimensionality. If the consumer searches for resources (by flying, swimming, or sitting and waiting) on habitat surfaces (for example, on the water surface, benthos or in grassland), the interaction is 2D, and if it searches habitat volume, the interaction is 3D. A consumer or resource may be involved in both 2D and 3D interactions, corresponding to different consumer–resource combinations and foraging strategies.

[1]Department of Biomathematics, David Geffen School of Medicine, University of California, Los Angeles, California 90095-1766, USA. [2]School of Marine and Tropical Biology, James Cook University, Townsville QLD 4811, Australia. [3]Department of Ecology & Evolutionary Biology, University of California, Los Angeles, California 90095, USA. [4]Santa Fe Institute, 1399 Hyde Park Road, Santa Fe, New Mexico 87501, USA.

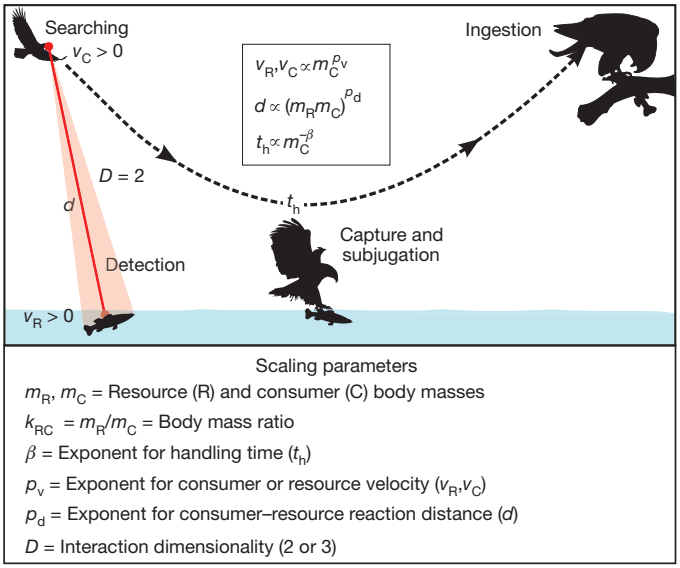

Figure 2 | Model for scaling of search and consumption rate with body size. This model (2D active capture is shown here) can also be used to predict search and consumption rates for grazing and sit-and-wait foraging strategies (Supplementary Information).

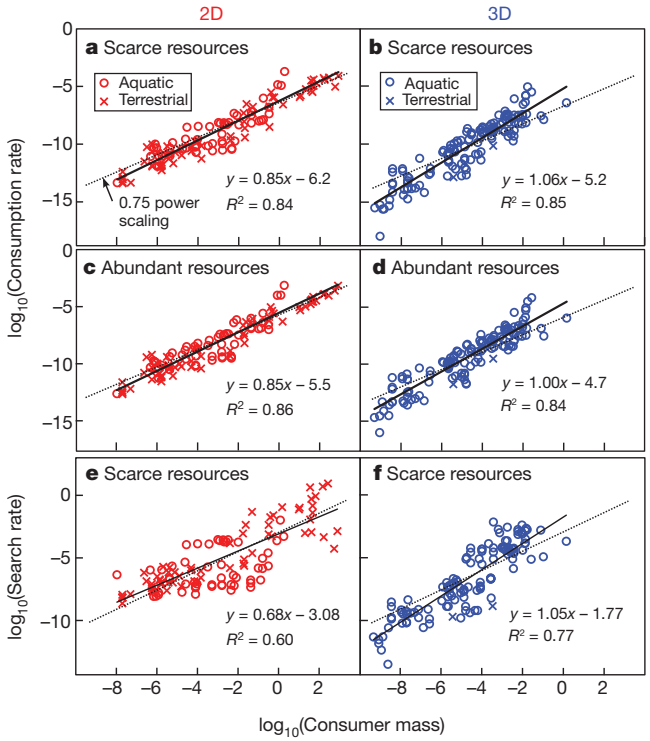

Figure 3 | Effect of interaction dimensionality on scaling of search and consumption rate. **a**–**d**, Scaling of per-capita consumption rate (kg s^{-1}) with consumer body mass (kg) at different resource densities. **e**, **f**, Scaling of search rate (m^2 s^{-1} in 2D, and m^3 s^{-1} in 3D). See Table 1 for sample sizes. Solid black lines were fitted using OLS regression (see Methods). Exponents in all panels except **e** are significantly different from the canonical 0.75 value (dotted line). Consumption-rate scaling shows less variance than search rate, possibly because consumers choose resources that maximize biomass consumption rate (product of search rate, resource density and resource mass; equation (4)), thus minimizing scatter.

Empirical patterns

Using our comprehensive data set, we first demonstrate strong empirical differences between 2D and 3D interactions in the scaling of search and consumption rate with consumer body size (Fig. 3). When resources are scarce, more closely resembling field conditions, the observed scaling exponent for consumption rate in 3D interactions (1.06 ± 0.06 (95% confidence intervals)) is significantly higher than in 2D (0.85 ± 0.05) (likelihood ratio test, $P < 0.001$) (Fig. 3a, c). These scaling exponents are significantly higher than the currently used exponent of 0.75 (one-sample F-test $P < 0.01$). Furthermore, apart from organisms that are much smaller than a honeybee (weighing less than 3×10^{-4} kg, where 2D and 3D scaling lines would intersect), 3D consumption rates are higher than in 2D (Fig. 3a, b). For a 1-kg organism, 3D consumption rate is ten times higher than in 2D (6.30 ± 3.01 versus 0.63 ± 0.24 mg s^{-1}) (Fig. 3a, b).

When resources are abundant, typical of laboratory conditions, consumption rates still scale more steeply (1.00 ± 0.06 versus 0.85 ± 0.05) and show higher baseline values in 3D than 2D (19.95 ± 11.00 versus 3.16 ± 1.30 mg s^{-1} for a 1-kg organism) (Fig. 3c, d). Thus, even at high resource densities at which searching for resources is expected to be less constraining, dimensionality remains important. The canonical 0.75 scaling exponent for consumption rate is excluded from the 95% confidence intervals of the observed scaling exponents under all conditions (Fig. 3).

We also analysed the scaling of search rates. The rate at which a consumer searches for a resource limits consumption rates when resources are scarce (Figs 1, 2 and 3e, f). For active-capture and grazing foragers, search rate (area/time or volume/time) is the speed at which a consumer moves through the landscape to find food, whereas for sit-and-wait foragers, it is the speed at which resources move through the consumer's attack space (Figs 1 and 2). We find that search rates have a scaling exponent of 1.05 ± 0.08 in 3D and 0.68 ± 0.12 in 2D (Fig. 3e, f), indicating that differences in consumption-rate scaling are primarily driven by differences in search rate. This result is a key validation of our model below.

A mechanistic model for search rate

Our empirical analysis reveals that search- and consumption-rate scaling vary systematically with the dimensionality of search space (that is, interaction dimensionality). We now present a model that predicts these empirical patterns by focusing on three key components of search rate: relative velocity, reaction distance and handling time[13,17,26] (Fig. 2). Relative velocity (v_r) is the rate at which consumer–resource pairs converge across the landscape, and it is the root-mean-square of their body velocities. A potential encounter occurs when either the resource or consumer comes within the distance (d) at which one can detect and react to the other. Because each individual moving through the landscape maintains a search space enclosed by a surface with radius d, we can derive (Supplementary Information) that the search rate (α) increases with dimensionality (D):

$$\alpha = s_D v_r d^{D-1} \quad (1)$$

where $s_D = 2$ in 2D and π in 3D. Based on biomechanical principles, we obtained predictions for the scaling exponents p_v and p_d (of v_r and d, respectively; Fig. 2), and validated them empirically using another, independent data set that we compiled (Table 1 and Supplementary Information). Using these, we predict:

$$\alpha = \alpha_0 m_C^{p_v + 2p_d(D-1)} f(k_{RC}) \quad (2)$$

where m_C is consumer body mass. For active foraging, the constant α_0 is $2v_0d_0$ in 2D and $\pi v_0 d_0^2$ in 3D. The function $f(k_{RC})$ isolates dependence of α on consumer–resource size ratio k_{RC} (that is, m_R/m_C (where m_R is resource body mass)) from its direct dependence on consumer mass. Both α_0 and $f(k_{RC})$ vary weakly with foraging strategy (Supplementary Information). To relate equation (2) directly to previous studies by expressing it solely in terms of consumer mass, we determine how k_{RC} scales with consumer mass using our consumption-rate data set. Substituting this scaling together with values for p_v and p_d (Table 1) into equation (2) gives:

Table 1 | Empirical and predicted scaling exponents of consumption rate and its components with interaction dimensionality (*D*)

D	Search and consumption rate (n = 255)			Consumption-rate components				
	Search rate (scarce resources)	Consumption rate		Relative velocity (n = 21)	Reaction distance (n = 39)	Handling time (n = 78)	Resource mass (n = 255)	Resource density (n = 255)
		Scarce resources	Abundant resources					
2D	**0.68** ± 0.12* (0.63)	**0.85** ± 0.05 (0.78)	**0.85** ± 0.05 (0.78)	0.26 ± 0.04* (0.27)	0.21 ± 0.08 (0.33)	−1.02 ± 0.08 (−0.75)	0.73 ± 0.10	−0.79 ± 0.08
3D	**1.05** ± 0.08* (1.03)	**1.06** ± 0.06 (1.16)	**1.00** ± 0.06 (1.16)	0.26 ± 0.04* (0.27)	0.20 ± 0.06 (0.33)	−1.1 ± 0.07 (−0.75)	0.92 ± 0.08	−0.86 ± 0.07

For search and consumption rate, if the 3D exponent is significantly larger than 2D as predicted (likelihood ratio test), both are shown in bold. There are no predicted exponents for resource mass and resource density scaling because they depend upon experimental design (Supplementary Information). Steeper than predicted exponents of handling time may arise because pursuit and subjugation scale with maximal rather than resting metabolic rate[8,21].

* Empirical exponent is statistically indistinguishable (P = 0.05 for all significance tests) from the predicted value (in parentheses).

$$\alpha \approx \alpha_{2D} m_C^{0.63} \text{ in 2D}$$
$$\alpha \approx \alpha_{3D} m_C^{1.03} \text{ in 3D} \quad (3)$$

where α_{2D} and α_{3D} are dimension-specific constants. These exponents match our empirical results extremely well (Fig. 3e, f and Table 1). Even if the weak contribution of $f(k_{RC})$ (Supplementary Information) to the scaling is ignored, the predicted search rate exponents ($p_v + 2p_d(D–1)$) would be 0.68 in 2D and 1.06 in 3D. These exponents are extremely close to the empirical estimates of 0.68 ± 0.12 in 2D and 1.05 ± 0.08 in 3D (Table 1; Fig. 3).

Predictions for consumption rate

The product of search rate, α, and resource density, x_R (individuals per area or volume), yields encounter rate. Consumption rate is constrained by this encounter rate and by handling time; that is, the duration of time to pursue, subdue and ingest each resource (Fig. 2). Together, these components give a saturating per-capita biomass consumption rate (c) (Holling's type II functional response[27]) in terms of spatial dimension (D):

$$c = \frac{\alpha m_R x_R}{1 + t_h \alpha m_R x_R} = \frac{s'_D v_r d^{D-1} m_R x_R}{1 + t_h s'_D v_r d^{D-1} m_R x_R} \quad (4)$$

Here, m_R is the average mass of the resource, $x_R m_R$ is resource biomass density, and t_h is conventional handling time divided by resource mass (Supplementary Information 1.4). The constant s'_D includes a roughly constant attack success probability. Our results are robust to changes in this probability for resource items common in the consumer's diet (Supplementary Information).

With scarce resources ($x_R \to x_{R,min}$) the second term in the denominator of equation (4) becomes much smaller than 1, and thus $c \approx \alpha x_R m_R$. Substituting the scaling for α (equation (2)) gives:

$$c = \alpha_0 m_C^{p_v + 2p_d(D-1)} f(k_{RC}) x_R m_R \quad (5)$$

To convert this into a scaling relationship solely with consumer mass, we use our functional response data set (Supplementary Information) to quantify the scaling of x_R and m_R with consumer mass (Table 1). Substituting these along with the previously determined scaling of size ratio (k_{RC}) in equation (5) gives:

$$c \approx c_{2D} m_C^{0.78} \text{ in 2D}$$
$$c \approx c_{3D} m_C^{1.16} \text{ in 3D} \quad (6)$$

where c_{2D} and c_{3D} are dimension-specific constants. Equation (6) predicts the steeper and superlinear scaling that is empirically observed in 3D for consumption rate (Fig. 3a, b and Table 1). Note that the scaling of consumption rate, c, closely matches the scaling of search rate, α (compare equations (3) and (6)). The existing small difference arises because of the weak scaling of the product ($x_R m_R$) of resource density and mass with consumer mass (Table 1 and Supplementary Information).

When resources are unlimited ($x_R \to \infty$), the term $s'_D v_r d^{D-1} x_R m_R$ dominates both the numerator and denominator of equation (4), resulting in a value of 1. Consequently, search and detection become instantaneous, and consumption rate depends only on mass-specific handling rate ($1/t_h$) (Fig. 2):

$$c = t_{h,0}^{-1} m_C^{\beta} \quad (7)$$

where β is the scaling exponent of the consumer's whole-body metabolic rate and $t_{h,0}$ is a body-temperature and metabolic-state-dependent constant. We find that mass-specific handling time, t_h, scales as 1.1 ± 0.07 in 3D and 1.02 ± 0.08 in 2D (Supplementary Information). However, the observed consumption-rate scaling in 2D is 0.85 ± 0.05, and is 1.00 ± 0.06 in 3D, both closer to predictions for scarce rather than unlimited resources (Table 1). Therefore, even when functional responses seem to saturate and resources are considered abundant, consumption rate does not scale like handling time, and must therefore continue to be constrained by search dimensionality. This also explains why most previous studies have reported 0.75 power scaling of consumption rate[7,8,19]. The data in these previous studies are actually maximal ingestion rates collected from sedentary individuals that are provided with unlimited resources[7,8,19]. Our data, for both scarce and abundant resources, are more representative of field conditions because they are extracted from functional response data.

Although our theory predicts that α_{3D} and c_{3D} are larger than α_{2D} and c_{2D}, respectively (Supplementary Information), the magnitude of the observed difference is much larger than predicted (Fig. 3). One explanation is that most 3D interactions are aquatic, and most 2D interactions are terrestrial. The energetic cost for swimming is about ten times lower than for running[18,19], probably increasing encounter rates for non-directed movement. This difference could elevate the intercept (but not exponent), contributing to the observed ten times larger baseline consumption rates in 3D. Nevertheless, 2D aquatic and 2D terrestrial interactions scale similarly (Fig. 3a–c), indicating other differences between pelagic (3D) and benthic (2D) aquatic zones, and highlighting the need for further study.

Dimensionality and trophic interaction strengths

By deriving the scaling of search rate (α), a fundamental parameter in consumer–resource and food-web models, we have provided a mechanistic basis for linking interaction dimensionality with trophic interaction strengths, which are proportional to $\alpha x_R m_R / m_C$ (refs 11, 13, 15, 16, 28, 29). In contrast to current theories, our results show that scaling of trophic interaction strength can deviate substantially from $m_C^{-0.25}$. Specifically, if resource size (m_R) and resource density (x_R) are decoupled from consumer size, consumption rate scales like search rate (equation (3)), and thus interaction strength scales as $\alpha x_R m_R / m_C \propto m_C^{-0.32}$ in 2D, and $m_C^{0.05}$ in 3D. Even when m_R and x_R scale with consumer mass (Table 1 and Supplementary Fig. 2), trophic interaction strengths scale as $m_C^{-0.15}$ (2D) or $m_C^{0.06}$ (3D) when resources are scarce, and as $m_C^{-0.15}$ (2D) or m_C^{0} (3D) when resources are abundant. This variation in the scaling of trophic interaction strengths implies that consumer–resource dynamics are likely to be constrained by interaction dimensionality.

Implications for population dynamics

By incorporating our scaling equations for α (equation (3)) into a population dynamics model (Methods), we now show that dimensionality can affect populations in three fundamental ways. First, 3D interactions allow a larger range of viable consumer–resource body-size

combinations than in 2D, primarily because 3D consumption rates scale more steeply and have higher baseline values. Depending upon baseline carrying capacity (K_0, defined as maximal biomass density for a 1 kg organism; Supplementary Information), the majority of 2,929 species pairs from seven communities fall within our predicted coexistence domains (Fig. 4a), with upper and lower limits of observed size ratios closely matching predicted extinction boundaries. In 2D, when K_0 ranges from 0.01 to 1 ($kg^{0.75}\,m^2$) the predicted coexistence domains contain 88.8% to 99.8% of the empirical data. In 3D, when K_0 ranges from 3 to 300 ($kg^{0.75}\,m^3$), 74.3% to 99.8% of the data are within the predicted domain (we explain below why carrying capacity is typically higher in 3D than 2D). Thus, interaction dimensionality may explain why consumer–resource interactions with larger size ratios (for example, filter feeding[30]) and larger consumers are more common in pelagic environments compared to benthic or terrestrial environments[1,8,31] (Fig. 4a).

Second, because strong trophic interactions can destabilize communities[15,16,28,29], communities dominated by 3D interactions (for example, pelagic or aerial habitats) may be inherently unstable. Indeed, we find that persistent consumer–resource boom–bust dynamics are more likely in 3D than in 2D (Fig. 4b and Supplementary Fig. 3). In nature, these instabilities may be partly offset by larger regions of coexistence that are possible in 3D (Fig. 4a) or by negative consumer density dependence[3,24]. Nevertheless, our results are consistent with empirical observations that pelagic communities appear less stable than terrestrial communities[5]. They also suggest that 3D aquatic ecosystems may experience more frequent top-down regulation than 2D terrestrial ecosystems[32,33].

Third, we predict that population densities across consumer–resource pairs scale with body size more steeply in 3D (exponent of −1.12) than 2D (exponent of −0.76) (Fig. 4c). Only 2D scaling matches Damuth's −0.75 rule, which was derived from data on terrestrial mammals (that is, 2D consumers)[14,34]. Thus, for a given carrying capacity (maximal abundance of resources), steeper size–abundance scaling of consumers in 3D habitats relative to 2D habitats should be expected, and this helps to explain deviations from Damuth's rule in local communities[6,14,34–36].

In our population model, we assume resource carrying capacities scale with a 0.75 exponent (Supplementary Information), as expected when food supply to resources is unlimited (equation (7))[26]. For example, maximal abundance of primary producers in 2D (for example, terrestrial plants) and 3D (for example, pelagic phytoplankton) should scale as metabolic rate (that is, Damuth's rule) irrespective of dimensionality, which is well supported empirically[6,8,37,38]. Future studies should incorporate potential differences in scaling of carrying capacity across trophic levels. We also assume higher baseline carrying capacities (K_0) in 3D than 2D (Fig. 4a) because pelagic (3D) phytoplankton have 2–3 orders of magnitude higher turnover rates than terrestrial plants and form a less variable and more nutritious autotroph base than plants in 2D terrestrial ecosystems such as grasslands[6,32,39]. This is an important difference between habitats because it helps to explain the potential advantage of 3D interactions. If resources had the same numbers (but not densities) in 2D and 3D habitats (for example, 1 kg m^{-2} and 1 kg m^{-3}), resources would probably be too sparse for a 3D search space to be advantageous.

The consequences of interaction dimensionality for population dynamics may also be mediated by other abiotic differences between aquatic and terrestrial habitats. For example, 2D habitats such as benthic zones may have a greater potential for prey refuges than 3D habitats such as pelagic zones. Structural complexity reduces consumer search rates, potentially resulting in type III functional responses instead of type I or II (refs 30, 40). We find no significant propensity for type III functional responses in 2D relative to 3D in our data set (Supplementary Information), probably because laboratory experiments typically use habitats that are simpler than real habitats. Even if type III responses are more common in 2D, results for the effects of dimensionality on consumer–resource population dynamics remain qualitatively unchanged (Supplementary Information). Nevertheless, an important future direction will be to understand how habitat complexity affects search and consumption rates. Synthesizing our model with previous work on fractal dimensionality of resource dispersion[3,22,25] should be an important step in this direction. Perception of structural complexity also scales with body size[3]. Grasslands may be structurally simple for a bison, but complex for a nematode.

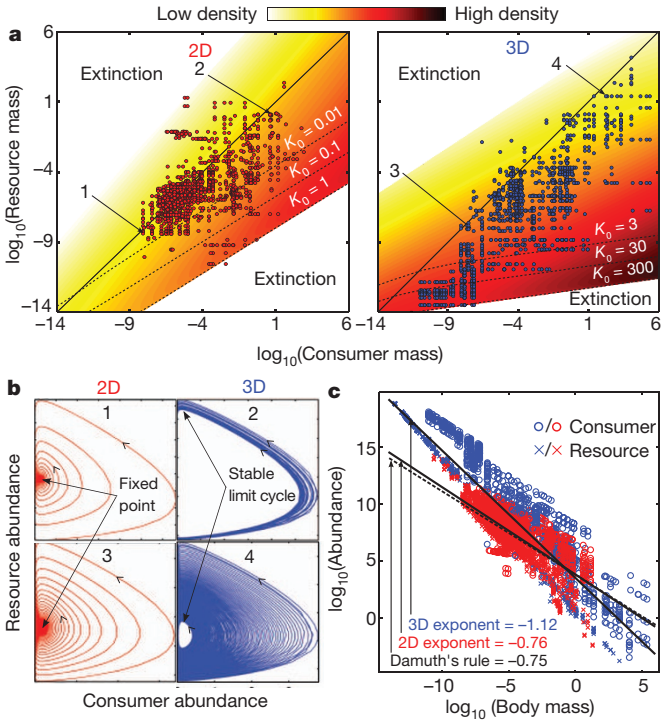

Figure 4 | Effects of interaction dimensionality on consumer–resource dynamics. a, Intensity map of logarithm of total consumer–resource equilibrium densities, ranging from coexistence at high (dark) to low (yellow) densities, or extinction (white). Black dots are real 2D (n = 1,627) and 3D (n = 1,302) consumer–resource pairs (Supplementary Table 8). Consumer and resource sizes are equal along the diagonal line. Lower extinction boundaries (dashed lines) correspond to different baseline carrying capacities (K_0); the outermost boundary corresponds to empirical estimates. Predicted 2D coexistence regions that lack observed species pairs probably represent undersampling of interactions for the smallest consumers (for example, micro predators) and largest consumers (for example, large mammalian herbivores)[31]. **b,** Comparison of population dynamics of two 2D (1 and 2 in **a**) and two 3D (3 and 4 in **a**) species pairs. **c,** Scaling of equilibrium abundance across all 3D (blue) and 2D (red) consumer–resource pairs plotted in **a**. The variation and discrete appearance of the data arises mainly because a consumer may feed on multiple resource species of different sizes and vice versa.

Conclusion

Our study provides new and more accurate scaling relationships for consumer–resource interactions[11,16,31], gives novel insights into consumer–resource dynamics, and offers a mechanistic model that incorporates dimensionality and foraging strategy into food-web dynamics. Our results help to explain why aquatic environments generally show higher energy fluxes and lower stability than terrestrial environments[5], why they often show inverted biomass pyramids[5,32], and why larger consumers have a relative advantage in pelagic (3D) versus terrestrial (2D) environments[1,6]. Predicting strengths of pair-wise trophic interactions is key to understanding higher-order effects, including indirect interactions and polyphagy[5,28,29]. Our model for pairwise interactions should provide a starting point for studying how the effects of dimensionality propagate through entire community food-webs. Studying communities with mixtures of 2D and 3D interactions will

be particularly revealing in this context. We conclude that interaction dimensionality is a critical factor driving consumer–resource dynamics. A better understanding of the effects of dimensionality will lead to better predictions of food-web and ecosystem dynamics, and how these complex systems might respond to environmental change.

METHODS SUMMARY

Functional response data were compiled from the literature (Supplementary Table 5). Interaction dimensionality was assigned according to consumer search space (Fig. 1). The minimum resource density in each study was classified as scarce, and the density corresponding to the maximum consumption rate was classified as abundant. The search rate (α) in each functional response was calculated at each scarce density by dividing the associated consumption rate (c) by the associated density. The scaling of α is our fundamental theoretical result (equation (2)) and is based on derived scalings for v_r, d and t_h. We verified predicted scalings of these components by compiling an additional data set of 136 interactions between 157 taxa. To move from predicted scaling exponents of α (equation (3)) to predictions for scaling exponents of c (equation (4)), we calculated the scaling of resource number density (x_R) and mass (m_R) across studies in the functional response database. All exponents were estimated using ordinary least squares regression (OLS) of log trait value versus log body mass. Major axis regression yields steeper exponents than OLS but does not qualitatively alter our results. We also tested for robustness of predictions to realistic variation in body velocity scaling. All data were standardized to 15 °C using the Boltzmann–Arrhenius model[9,14]. For population dynamics we used the Rosenzweig–MacArthur model for the rate of change in time, t, for the resource ($R = x_R m_R$) and consumer ($C = x_C m_C$) biomass densities[13,26]:

$$\frac{dR}{dt} = rR\left(1 - \frac{R}{K}\right) - \frac{(\alpha/m_C)RC}{1 + t_h \alpha R}$$

$$\frac{dC}{dt} = \frac{e(\alpha/m_C)RC}{1 + t_h \alpha R} - zC$$

Here, r is the resource's intrinsic biomass production rate, K is resource's biomass carrying capacity, z is the consumer's biomass loss rate, e is the consumer's biomass conversion efficiency, and t_h is the resource mass-specific handling time. Size scaling for α and t_h were based on our results, and that for r, z and K were based on previous work[8,9,14]. We tested robustness of our results by varying model structure between the Rosenzweig-MacArthur model and the Lotka–Volterra predator–prey model, and also by using a type III instead of a type II functional response.

Received 13 December 2011; accepted 3 April 2012.
Published online 30 May 2012.

1. Cohen, J. E. & Fenchel, T. Marine and continental food webs: three paradoxes? *Phil. Trans. R. Soc. Lond. B* **343,** 57–69 (1994).
2. Savage, V. M., Webb, C. T. & Norberg, J. A general multi-trait-based framework for studying the effects of biodiversity on ecosystem functioning. *J. Theor. Biol.* **247,** 213–229 (2007).
3. Ritchie, M. E. *Scale, Heterogeneity, and the Structure and Diversity of Ecological Communities*. Vol. 112 (Princeton Univ. Press, 2009).
4. Briand, F. & Cohen, J. E. Environmental correlates of food-chain length. *Science* **238,** 956–960 (1987).
5. Rip, J. M. K. & McCann, K. S. Cross-ecosystem differences in stability and the principle of energy flux. *Ecol. Lett.* **14,** 733–740 (2011).
6. Cyr, H., Peters, R. H. & Downing, J. A. Population density and community size structure: comparison of aquatic and terrestrial systems. *Oikos* **80,** 139–149 (1997).
7. Farlow, J. O. A consideration of the trophic dynamics of a late Cretaceous large-dinosaur community (Oldman formation). *Ecology* **57,** 841–857 (1976).
8. Peters, R. H. *The Ecological Implications of Body Size*. (Cambridge Univ. Press, 1983).
9. Brown, J. H., Gillooly, J. F., Allen, A. P., Savage, V. M. & West, G. B. Toward a metabolic theory of ecology. *Ecology* **85,** 1771–1789 (2004).
10. Otto, S. B., Rall, B. C. & Brose, U. Allometric degree distributions facilitate food-web stability. *Nature* **450,** 1226–1229 (2007).
11. Berlow, E. L. *et al.* Simple prediction of interaction strengths in complex food webs. *Proc. Natl Acad. Sci. USA* **106,** 187–191 (2009).
12. Lewis, H. M., Law, R. & McKane, A. J. Abundance–body size relationships: the roles of metabolism and population dynamics. *J. Anim. Ecol.* **77,** 1056–1062 (2008).
13. Yodzis, P. & Innes, S. Body size and consumer resource dynamics. *Am. Nat.* **139,** 1151–1175 (1992).
14. Savage, V. M., Gillooly, J. F., Brown, J. H., West, G. B. & Charnov, E. L. Effects of body size and temperature on population growth. *Am. Nat.* **163,** 429–441 (2004).
15. Brose, U., Williams, R. J. & Martinez, N. D. Allometric scaling enhances stability in complex food webs. *Ecol. Lett.* **9,** 1228–1236 (2006).
16. Brose, U. Body-mass constraints on foraging behaviour determine population and food-web dynamics. *Funct. Ecol.* **24,** 28–34 (2010).
17. McGill, B. J. & Mittelbach, G. G. An allometric vision and motion model to predict prey encounter rates. *Evol. Ecol. Res.* **8,** 691–701 (2006).
18. Alexander, R. M. *Principles of Animal Locomotion*. (Princeton Univ. Press, 2003).
19. Schmidt-Nielsen, K. *Scaling, Why is Animal Size so Important?* (Cambridge Univ. Press, 1984).
20. Jetz, W., Carbone, C., Fulford, J. & Brown, J. H. The scaling of animal space use. *Science* **306,** 266–268 (2004).
21. Weibel, E. R., Bacigalupe, L. D., Schmitt, B. & Hoppeler, H. Allometric scaling of maximal metabolic rate in mammals: muscle aerobic capacity as determinant factor. *Respir. Physiol. Neurobiol.* **140,** 115–132 (2004).
22. Holling, C. S. Cross-scale morphology, geometry, and dynamics of ecosystems. *Ecol. Monogr.* **62,** 447–502 (1992).
23. Whitehead, H. & Walde, S. J. Habitat dimensionality and mean search distances of top predators: implications for ecosystem structure. *Theor. Popul. Biol.* **42,** 1–9 (1992).
24. Witting, L. The body mass allometries as evolutionarily determined by the foraging of mobile organisms. *J. Theor. Biol.* **177,** 129–137 (1995).
25. Milne, B. T., Turner, M. G., Wiens, J. A. & Johnson, A. R. Interactions between the fractal geometry of landscapes and allometric herbivory. *Theor. Popul. Biol.* **41,** 337–353 (1992).
26. Weitz, J. S. & Levin, S. A. Size and scaling of predator-prey dynamics. *Ecol. Lett.* **9,** 548–557 (2006).
27. Holling, C. S. Some characteristics of simple types of predation and parasitism. *Can. Entomol.* **91,** 385–398 (1959).
28. Laska, M. S. & Wootton, T. J. Theoretical concepts and empirical approaches to measuring interaction strength. *Ecology* **79,** 461–476 (1998).
29. Pawar, S. Community assembly, stability and signatures of dynamical constraints on food web structure. *J. Theor. Biol.* **259,** 601–612 (2009).
30. Jeschke, J. M., Kopp, M. & Tollrian, R. Consumer-food systems: why type I functional responses are exclusive to filter feeders. *Biol. Rev. Camb. Phil. Soc.* **79,** 337–349 (2004).
31. Brose, U. *et al.* Consumer–resource body-size relationships in natural food webs. *Ecology* **87,** 2411–2417 (2006).
32. Shurin, J. B., Gruner, D. S. & Hillebrand, H. All wet or dried up? Real differences between aquatic and terrestrial food webs. *Proc. R. Soc. B* **273,** 1–9 (2006).
33. Chase, J. M. Are there real differences among aquatic and terrestrial food webs? *Trends Ecol. Evol.* **15,** 408–412 (2000).
34. Damuth, J. Population density and body size in mammals. *Nature* **290,** 699–700 (1981).
35. Reuman, D. C. *et al.* Allometry of body size and abundance in 166 food webs. *Adv. Ecol. Res.* **41,** 1–44 (2009).
36. Leaper, R. & Raffaelli, D. Defining the abundance body-size constraint space: data from a real food web. *Ecol. Lett.* **2,** 191–199 (1999).
37. Cermeño, P., Maranon, E., Harbour, D. & Harris, R. P. Invariant scaling of phytoplankton abundance and cell size in contrasting marine environments. *Ecol. Lett.* **9,** 1210–1215 (2006).
38. Belgrano, A., Allen, A. P., Enquist, B. J. & Gillooly, J. F. Allometric scaling of maximum population density: a common rule for marine phytoplankton and terrestrial plants. *Ecol. Lett.* **5,** 611–613 (2002).
39. Field, C. B., Behrenfeld, M. J., Randerson, J. T. & Falkowski, P. Primary production of the biosphere: integrating terrestrial and oceanic components. *Science* **281,** 237–240 (1998).
40. Vucic-Pestic, O., Rall, B. C., Kalinkat, G. & Brose, U. Allometric functional response model: body masses constrain interaction strengths. *J. Anim. Ecol.* **79,** 249–256 (2010).

Supplementary Information is linked to the online version of the paper at www.nature.com/nature.

Acknowledgements We thank the authors who contributed data (Supplementary Tables 5–8), and P. Amarasekare, J. H. Brown, E. Economo, A. Mikheyev, C. Estrada, C. Johnson, M. Johnson and K. Lafferty for helpful discussions and comments. S.P., A.I.D. and V.M.S. were supported by University of California, Los Angeles Biomathematics start-up funds and by the US National Science Foundation Division of Environmental Biology award 1021010. The data reported in this paper are available in the Supplementary Information online.

Author Contributions S.P., A.I.D. and V.M.S. contributed equally to this work. All authors discussed the results and commented on the manuscript.

Author Information Reprints and permissions information is available at www.nature.com/reprints. The authors declare no competing financial interests. Readers are welcome to comment on the online version of this article at www.nature.com/nature. Correspondence and requests for materials should be addressed to S.P. (samraat@ucla.edu).